Polymer Journal, Vol. 39, No. 8, pp. 792–801 (2007)

Wormlike Micelles of Hexaoxyethylene Decyl $C_{10}E_6$ and Tetradecyl $C_{14}E_6$ Ethers Containing *n*-Dodecanol

Yoshiyuki EINAGA,† Megumi EBIHARA, and Ritsuko UCHIDA

Department of Chemistry, Nara Women's University, Kitauoyanishi-machi, Nara 630-8506, Japan

(Received April 5, 2007; Accepted May 2, 2007; Published June 19, 2007)

ABSTRACT: Wormlike micelles formed with the surfactant hexaoxyethylene decyl $C_{10}E_6$ and tetradecyl $C_{14}E_6$ ethers were studied by static (SLS) and dynamic light scattering (DLS) experiments to examine variation of the micellar characteristics with uptake of *n*-dodecanol. The SLS results have been analyzed by the light scattering theory for micelle solutions to yield the molar mass $M_w(c)$ as a function of concentration c along with the cross-sectional diameter d of the micelle. The apparent hydrodynamic radius $R_{H,app}(c)$ determined by DLS as a function of c is also successfully analyzed by a fuzzy cylinder theory which takes into account the hydrodynamic and direct collision interactions among micelles, allowing us to evaluate the stiffness parameter λ^{-1}. It has been found that the micellar length increases with increasing surfactant weight fraction w_s or with raising temperature T irrespective of the composition of *n*-dodecanol content in the micelles. The length of the micelles at fixed w_s and T steeply increases with increasing weight fraction w_d of *n*-dodecanol. The length of the $C_{14}E_6$ micelles is extremely larger than that of the $C_{10}E_6$ micelles. The values of d and λ^{-1} are found to increase with increasing w_d. It has been found that the increase in λ^{-1} is more significant for the micelles of the surfactant molecules with shorter hydrophobic chain length. [doi:10.1295/polymj.PJ2007004]

KEY WORDS Wormlike Micelle / Light Scattering / Radius of Gyration / Diffusion Coefficient / Hydrodynamic Radius / Surfactant / Polyoxyethylene Alkyl Ether /

In the previous work on micellar solutions of nonionic surfactant polyoxyethylene alkyl ethers $H(CH_2)_i(OCH_2CH_2)_jOH$ (abbreviated C_iE_j) and their binary mixtures, we have studied characteristics of the micelles by static (SLS) and dynamic light scattering (DLS) measurements and viscometry.[1–9] It has been demonstrated that the SLS results (Rayleigh ratios) as a function of surfactant concentration are well represented by a molecular thermodynamic theory[10,11] formulated with the wormlike spherocylinder model to yield the values of $M_w(c)$ at a specified surfactant concentration c along with the cross-sectional diameter d of the micelles. The molar mass M_w dependence of the mean-square radius of gyration $\langle S^2 \rangle$, hydrodynamic radius R_H, and intrinsic viscosity $[\eta]$ is quantitatively represented by the chain statistical[12] and hydrodynamic[13–16] theories based on the wormlike chain and spherocylinder models, respectively, thereby providing us with the values of the stiffness parameter λ^{-1}.

Following the work, We have also studied $C_{12}E_6$, $C_{10}E_5$, and $C_{12}E_5$ micelles containing *n*-dodecanol to explore effects of uptake *n*-alcohol into the micelles on the micellar characteristics.[17–19] It has been then found that the SLS and DLS results are successfully analyzed as in the case of the micelle solutions of simple C_iE_j or their binary mixtures. In particular, it has been demonstrated that the fuzzy cylinder theory[20–22] is applied in a favorable way to analyze the apparent hydrodynamic radius $R_{H,app}$ as a function of the micelle concentration, thereby obtaining the concentration-dependent micellar growth by separating contributions of the enhancement of hydrodynamic interactions among micelles.

The present work extends the studies to micelles in the $C_{10}E_6$ + *n*-dodecanol + water and $C_{14}E_6$ + *n*-dodecanol + water systems. The main aim is to investigate effects of hydrophobic chain length of the surfactant molecules on the variation of the micellar characteristics such as the micellar length L, cross-sectional diameter d, and stiffness λ^{-1} with uptake of *n*-dodecanol.

EXPERIMENTAL SECTION

Materials

The surfactant $C_{10}E_6$ and $C_{14}E_6$ samples and *n*-dodecanol were purchased from Nikko Chemicals Co. Ltd. and Nakaraitesque Co., respectively, and used without further purification. The solvent water used was high purity (ultrapure) water prepared with Simpli Lab water purification system of Millipore Co.

Phase Diagram

Cloud-point temperature of a given micelle solution was determined as the temperature at which the intensity of the laser light transmitted through the solution abruptly decreased when temperature was gradually raised.

†To whom correspondence should be addressed (E-mail: einaga@cc.nara-wu.ac.jp).

$C_{10}E_6$ and $C_{14}E_6$ micelle solutions were prepared by dissolving respective surfactant in water with adding appropriate amount of *n*-dodecanol with a microliter syringe (Hamilton). Complete mixing and micelle formation were achieved by stirring the solutions using a magnetic stirrer for at least one day. *n*-Dodecanol is substantially insoluble in water and thus completely incorporated into the micelles. The weight fractions w of micelle solutions were determined gravimetrically and converted to mass concentrations c by the densities ρ of the solutions given below. Throughout this paper, w and c denote the weight fraction and mass concentration of $C_{10}E_6$ or $C_{14}E_6$ + *n*-dodecanol mixture in the $C_{10}E_6$ or $C_{14}E_6$ + water + *n*-dodecanol ternary solutions. *n*-Dodecanol content in the $C_{10}E_6$ or $C_{14}E_6$ + *n*-dodecanol mixture is represented by its weight fraction w_d.

Static Light Scattering

The scattering intensities were measured for micelle solutions of various w_d at 40.0 °C and for those of $w_d = 0.0704$ at 30.0, 35.0, and 40.0 °C for the system $C_{10}E_6$ + *n*-dodecanol + water, and for micelle solutions of various w_d at 25.0 °C and for those of $w_d = 0.0200$ at 15.0, 20.0, and 25.0 °C for the system $C_{14}E_6$ + *n*-dodecanol + water. The ratio $Kc/\Delta R_\theta$ was obtained for each solution as a function of the scattering angle θ ranging from 30 to 150° and extrapolated to zero scattering angle to evaluate $Kc/\Delta R_0$. Here, c is the mass concentration of surfactant + *n*-dodecanol, ΔR_θ is the excess Rayleigh ratio, and K is the optical constant defined as

$$K = \frac{4\pi^2 n^2 (\partial n/\partial c)_{T,p}^2}{N_A \lambda_0^4} \tag{1}$$

with N_A being the Avogadro's number, λ_0 the wavelength of the incident light in vacuum, n the refractive index of the solution, $(\partial n/\partial c)_{T,p}$ the refractive index increment, T the absolute temperature, and p the pressure. The plot of $Kc/\Delta R_\theta$ *vs.* $\sin^2(\theta/2)$ affords a good straight line for all the micelle solutions studied.

The apparatus used is an ALV DLS/SLS-5000/E light scattering photogoniometer and correlator system with vertically polarized incident light of 632.8 nm wavelength from a Uniphase Model 1145P He-Ne gas laser.

The micellar solutions were prepared in the same way as those for the cloud-point measurements described above. The experimental procedure is the same as described before.[1–5,7–9,18,19] In the present study, we have treated the micelle solutions as the binary system which consists of micelles containing *n*-dodecanol as a solute and water as a solvent.

The results for the refractive index increment $(\partial n/\partial c)_{T,p}$ measured at 632.8 nm with a Union Giken R601 differential refractometer are summarized as (in cm^3/g):

For the system $C_{10}E_6$ + *n*-dodecanol + water at 20.0 °C ≤ T ≤ 40.0 °C,

$$(\partial n/\partial c)_{T,p} = 0.133 - 2.43 \times 10^{-4}(T - 273.15) \quad (w_d = 0.0306) \tag{2}$$

$$(\partial n/\partial c)_{T,p} = 0.131 - 2.17 \times 10^{-4}(T - 273.15) \quad (w_d = 0.0505) \tag{3}$$

$$(\partial n/\partial c)_{T,p} = 0.133 - 2.25 \times 10^{-4}(T - 273.15) \quad (w_d = 0.0704) \tag{4}$$

For the system $C_{14}E_6$ + *n*-dodecanol + water at 15.0 °C ≤ T ≤ 25.0 °C,

$$(\partial n/\partial c)_{T,p} = 0.140 - 3.58 \times 10^{-4}(T - 273.15) \quad (w_d = 0.0195) \tag{5}$$

$$(\partial n/\partial c)_{T,p} = 0.140 - 3.75 \times 10^{-4}(T - 273.15) \quad (w_d = 0.0368) \tag{6}$$

$$(\partial n/\partial c)_{T,p} = 0.124 - 3.13 \times 10^{-4}(T - 273.15) \quad (w_d = 0.0406) \tag{7}$$

$$(\partial n/\partial c)_{T,p} = 0.127 - 1.85 \times 10^{-4}(T - 273.15) \quad (w_d = 0.0505) \tag{8}$$

Dynamic Light Scattering

DLS measurements were carried out to determine the translational diffusion coefficient D for the micelles by the use of the same apparatus and light source as used in the SLS studies described above. All the test solutions studied are the same as those used in the SLS studies. From the D values obtained by the cumulant method for the normalized autocorrelation function $g^{(2)}(t)$, the apparent hydrodynamic radius $R_{H,app}$ has been evaluated by the defining equation[18,23–25]

$$D = \frac{(1 - vc)^2 M_w k_B T}{6\pi\eta_0 R_{H,app}} \left(\frac{Kc}{\Delta R_0}\right) \tag{9}$$

where v is the partial specific volume of the solute (micelle), k_B is the Boltzmann constant, and η_0 is the solvent viscosity. It is to be noted that since the micelles observed may have a range of sizes, the values of D and $R_{H,app}$ should be regarded as an average.

Density

For all the micelle solutions containing *n*-dodeca-

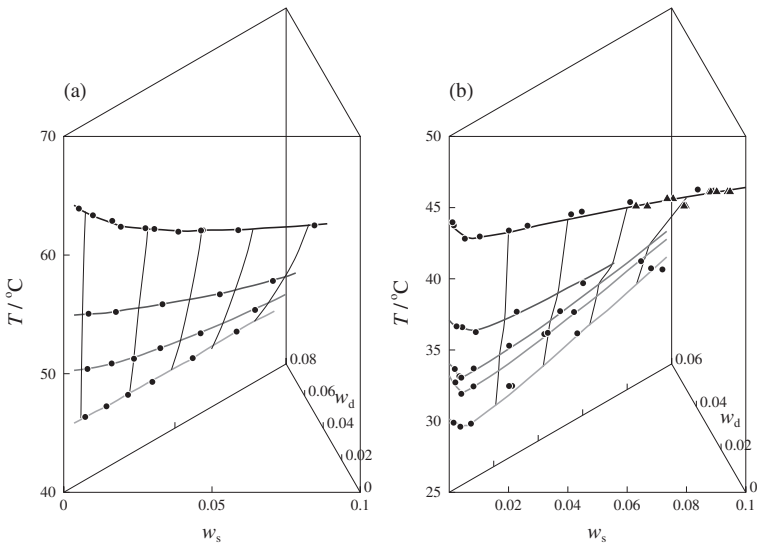

Figure 1. Three-dimensional representation of the binodal surface for the $C_{10}E_6$ + *n*-dodecanol + water (a) and $C_{14}E_6$ + *n*-dodecanol + water (b) systems: w_s, weight fraction of $C_{10}E_6$ or $C_{14}E_6$ in the solution; w_d, weight fraction of *n*-dodecanol in the $C_{10}E_6$ or $C_{14}E_6$ + *n*-dodecanol mixture. The data points for $w_d = 0$ in (a) and (b) are the literature results of Ref 3 and 1, respectively. Thick solid curves represent the results with increasing order of w_d from top to bottom, respectively.

nol, the solution density ρ has been found to be independent of micelle weight fraction w and *n*-dodecanol content w_d at any temperature examined. Thus we have used the literature values of the density ρ_0 of pure water at corresponding temperatures for ρ, and the values of v of the micelles have been calculated as ρ_0^{-1}.

RESULTS

Phase Behavior

Figure 1a and b represent 3D phase diagrams for the ternary systems $C_{10}E_6$ + *n*-dodecanol + water and $C_{14}E_6$ + *n*-dodecanol + water, respectively, constructed from the cloud point data, where the literature results at $w_d = 0$ are reproduced from Ref 3 and 1. Here, w_s is the weight fraction of the surfactant $C_{10}E_6$ or $C_{14}E_6$ in the solution. The phase boundaries shift to lower temperatures as w_d increases and the temperature shift with w_d is more significant at lower w_s. All the light scattering experiments have been performed in the L_1 phase below the binodal surface.

DISCUSSION

Analysis of SLS Data

As mentioned in the Introduction, we have analyzed the present SLS data by employing Sato theory for static light-scattering from micellar solutions[10,11] with wormlike spherocylinder model in order to determine M_w of the micelles as a function of c. The model consists of a wormlike cylinder of contour length $L - d$ with cross-sectional diameter d and two hemispheres of diameter d which cap both ends of the cylinder, and stiffness of the wormlike cylinder is represented by the stiffness parameter λ^{-1}. In the theory, the weight-average molar mass M_w of the micelles and its distribution have been formulated on the basis of multiple equilibria among various micelles of different sizes and monomer, by representing chemical potentials of the micelles as functions of c in a similar fashion to the classical mean-field and recent molecular theoretical approaches.[26–28] Here, the free-energy parameter g_2, which represents the difference in free energy between the surfactant molecules located in the end-capped portion to those in the central cylindrical portion in the micelles, plays a dominant role in the multiple equilibria and then the micellar growth with concentration. The intermicellar thermodynamic interactions have also been taken into account in the chemical potential on the basis of a statistical thermodynamic theory for stiff polymer solutions with the wormlike spherocylinder model.[11] The apparent virial coefficient $A(c)$, which includes the second A_2, third A_3, and higher virial coefficient terms, has been formulated to describe thermodynamic properties of micelle solutions up to high concentrations by taking into account the hard-core repulsive interactions dominated by the parameter d together with the attractive interactions dominated by the parameter $\hat{\epsilon}$ (the depth of the attractive potential well) among the micelles.

To sum up, the functions $M_w(c)$ and $A(c)$, and then the excess zero-angle Rayleigh ratio ΔR_0, have been formulated as functions of c with including d, g_2, and $\hat{\epsilon}$ as parameters. With the aid of the formulation, we

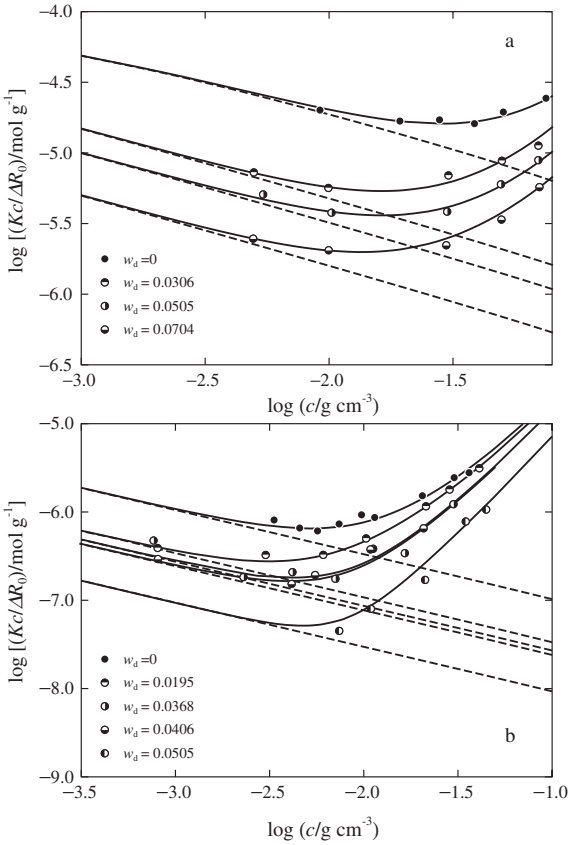

Figure 2. Bilogarithmic plots of $(Kc/\Delta R_0)$ against c for the $C_{10}E_6$ + *n*-dodecanol + water system ($T = 40.0\,^{\circ}C$) (a) and for the $C_{14}E_6$ + *n*-dodecanol + water system ($T = 25.0\,^{\circ}C$) (b) at various w_d indicated: filled circles for $w_d = 0$ in (a) and (b) are the literature results of Ref 3 and 1, respectively. The solid and dashed lines represent the theoretical values for $Kc/\Delta R_0$ and $1/M_w(c)$, respectively.

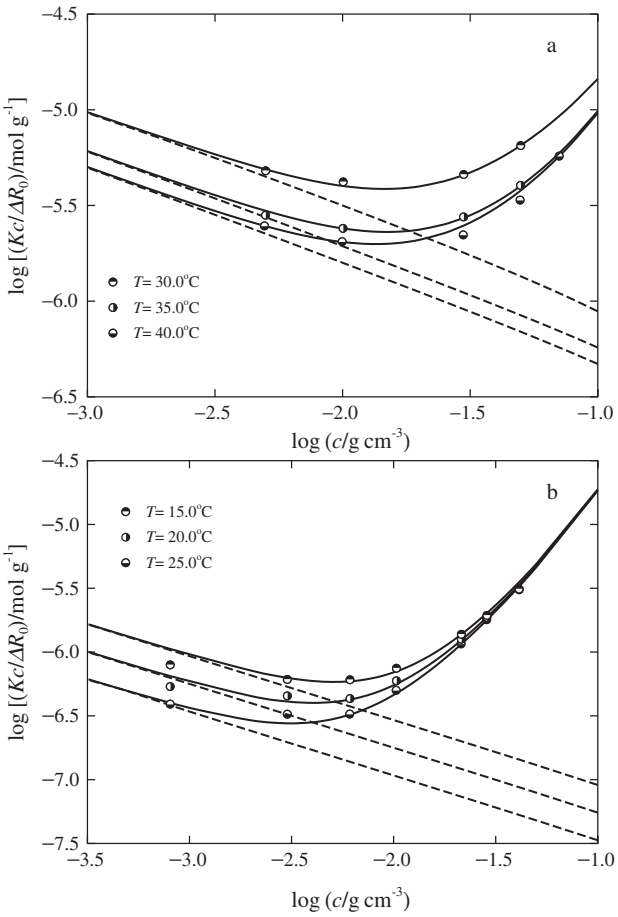

Figure 3. Bilogarithmic plots of $(Kc/\Delta R_0)$ against c for the $C_{10}E_6$ + *n*-dodecanol + water system of $w_d = 0.0704$ (a) and for the $C_{14}E_6$ + *n*-dodecanol + water system of $w_d = 0.0195$ (b) at various T indicated: the solid and dashed lines represent the theoretical values for $Kc/\Delta R_0$ and $1/M_w(c)$, respectively.

are able to evaluate $M_w(c)$ by determining the best-fit theoretical values of $Kc/\Delta R_0$ as a function of c to the observed data at fixed T with selected proper values of d, g_2, and $\hat{\epsilon}$. As in the case of the previous work,[18,19] we have treated present micelle solutions as two component systems consisting of micelles and solvent, although they include three components: surfactant $C_{10}E_6$ or $C_{14}E_6$, *n*-dodecanol, and water. It has been assumed in the analyses that the composition of $C_{10}E_6$ or $C_{14}E_6$ + *n*-dodecanol in the micelles is given by w_d. The weight average molecular weight of the $C_{10}E_6$ or $C_{14}E_6$ + *n*-dodecanol mixture calculated with a given w_d was used as the surfactant molecular weight M_0 required in the theoretical analysis.

Figure 2a and b demonstrate the results of curve-fitting for the solutions of the $C_{10}E_6$ micelles of various w_d indicated at $40.0\,^{\circ}C$ (a) and those of the $C_{14}E_6$ micelles at $25.0\,^{\circ}C$ (b), respectively. Figure 3a and 3b show the results for the solutions of the $C_{10}E_6$ micelles of $w_d = 0.0704$ at various T (a) and those of the $C_{14}E_6$ micelles of $w_d = 0.0195$ at various T (b), respectively. It is seen in Figure 3b that the data points at different T merge into a single composite line at large c. The results may imply that the $C_{14}E_6$ micelles containing *n*-dodecanol in this c range are large enough for their solutions to approach the moderately concentrated or semiconcentrate solutions. In this connection, it should be noted that for c approaching the range of moderately concentrated solutions, $Kc/\Delta R_0$ for real polymer solutions approaches proportionality with c^2, independent of the molecular weight.[29,30]

The solid curves in Figures 2 and 3 well coincide with the respective data points at given w_d or T, implying that the micelles containing *n*-dodecanol are well represented by the wormlike spherocylinder model. The dashed lines represent the values of $1/M_w(c)$ at respective w_d or T. For all the $C_{10}E_6$ and $C_{14}E_6$ micelles at any fixed w_d and T, they are straight lines with a slope of -0.5, showing that M_w increases with c following a relation $M_w \propto c^{1/2}$ in the range of c examined, as in the case of the previous findings for

the micelles formed with single surfactant of various type,[1–5,7] for those formed with binary C_iE_j mixtures,[8,9] and the $C_{10}E_5$ and $C_{12}E_5$ micelles containing *n*-dodecanol.[18,19] These results well agree with simple theoretical predictions derived from the thermodynamic treatments of multiple equilibria among micelles of various aggregation numbers.[10,26–28] The increase in $M_w(c)$ with increasing c and w_d and with raising temperature is consistent with our previous results for the $C_{10}E_5$ + *n*-dodecanol and $C_{12}E_5$ + *n*-dodecanol micelles.[18,19] The solid and dashed curves coincide with each other at small c but the former rapidly increases with increasing c, deviating upward from the latter, indicating that contributions of the virial coefficient terms to $Kc/\Delta R_0$ are negligible at small c but progressively increase with increasing c as expected.

The d value determined by the curve fitting was independent of T but gradually increased with w_d for both $C_{10}E_6$ and $C_{14}E_6$ micelles containing *n*-dodecanol. They were 2.60, 2.80, 3.20, and 3.68 nm at w_d = 0, 0.0306, 0.0505, and 0.0704, respectively, for the former micelles and 2.40, 2.45, 2.58, 2.61, and 3.20 nm at $w_d = 0$, 0.0195, 0.0368, 0.0406, and 0.0505, respectively, for the latter. In these, the values at $w_d = 0$ are the literature results.[1,3]

Mean-Square Radius of Gyration

On the basis of the fundamental light-scattering equation for dilute polymer solutions

$$\frac{Kc}{\Delta R_\theta} = \left(\frac{1}{M_w} + 2A_2c + \cdots\right) + \left(\frac{\langle S^2\rangle}{3M_w}q^2 + \cdots\right) \tag{10}$$

$$q = \frac{4\pi n}{\lambda_0}\sin(\theta/2) \tag{11}$$

we have determined the apparent mean-square radius of gyration $\langle S^2\rangle_{app}$ for the $C_{14}E_6$ micelles containing *n*-dodecanol at finite c and w_d from the slope of the $Kc/\Delta R_\theta$ versus $\sin^2(\theta/2)$ plot. Here, $\langle S^2\rangle$ is the mean-square radius of gyration, q is the magnitude of the scattering vector, and λ_0 is the wave length of the incident light in vacuum. In the evaluation, we used the M_w values determined as described above at given c, w_d, and T. Since $\langle S^2\rangle$ is possibly affected by intermicellar interactions, it is denoted by $\langle S^2\rangle_{app}$. We note that the $\langle S^2\rangle_{app}$ values of the $C_{10}E_6$ micelles are not large enough to be determined by SLS measurements.

Molar mass dependence of $\langle S^2\rangle_{app}^{1/2}$ is exhibited in Figure 4a and b for the micelles with various w_d indicated at 25.0 °C (a) and for those with $w_d = 0.0195$ at various T (b). The data points for each fixed w_d form a single curve, independent of c and T,

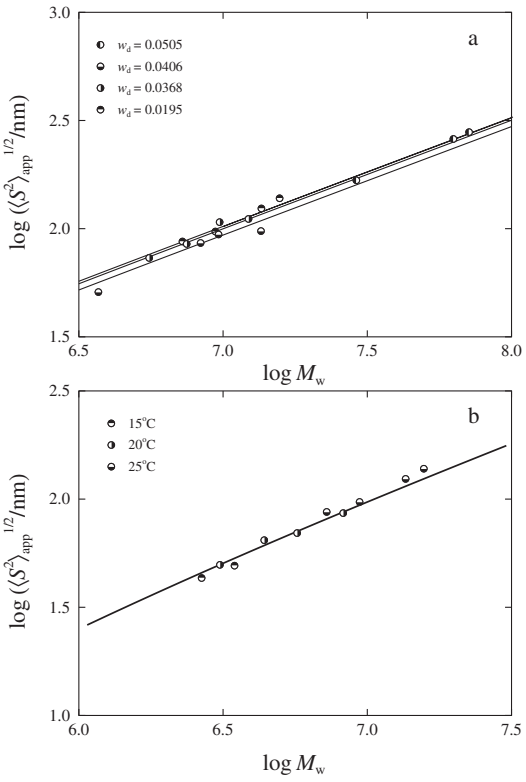

Figure 4. Bilogarithmic plots of $\langle S^2\rangle_{app}^{1/2}$ against M_w for the $C_{14}E_6$ + *n*-dodecanol + water system with various w_d indicated at $T = 25.0$ °C (a) and with $w_d = 0.0195$ at various T indicated (b). The solid lines represent the theoretical values.

implying that they correspond to the values for the isolated micelles, *i.e.*, $\langle S^2\rangle^{1/2}$. The observed results are quantitatively represented by the theoretical values of $\langle S^2\rangle^{1/2}$ calculated by Benoit-Doty equation for wormlike polymers[12] as shown by the solid curves. Here, the relation between M_w and the weight-average micellar length L_w derived from the micellar volume

$$L_w = \frac{4vM_w}{\pi N_A d^2} + \frac{d}{3} \tag{12}$$

has been utilized (L_w was used in place of L). In the calculation, the d values obtained from SLS results in the preceding section were used and then the λ^{-1} values were determined as 18, 19, 17, and 31 nm for $w_d = 0.0195$, 0.0368, 0.0406, and 0.0505, respectively, to achieve the best fit to the experimental results. It should be noted that the data points at different T in Figure 4b form a single composite curve reflecting the fact that the values of d and λ^{-1} are independent of T.

Hydrodynamic Radius of the Micelles

Figure 5a and b depict bilogarithmic plots of $R_{H,app}$ determined by eq 9 against c for the $C_{10}E_6$ + *n*-dodecanol micelles of various w_d at 40.0 °C and the $C_{14}E_6$ + *n*-dodecanol micelles of various w_d at

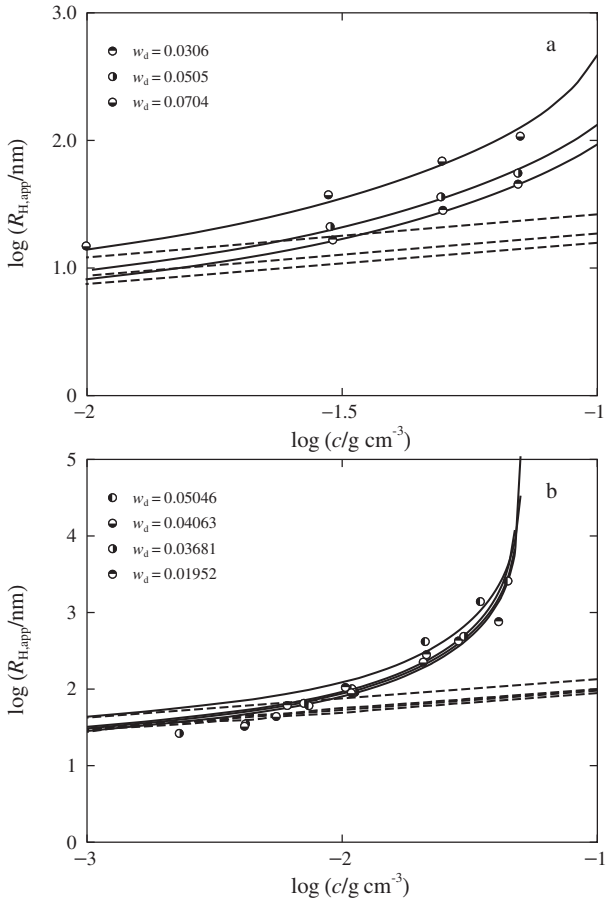

Figure 5. Bilogarithmic plots of $R_{H,app}$ against c for the $C_{10}E_6$ + n-dodecanol + water system ($T = 40.0\,^{\circ}C$) (a) and for the $C_{14}E_6$ + n-dodecanol + water system ($T = 25.0\,^{\circ}C$) (b) at various w_d indicated: the solid and dashed lines represent the theoretical values of $R_{H,app}$ and R_H for the isolated micelles, respectively.

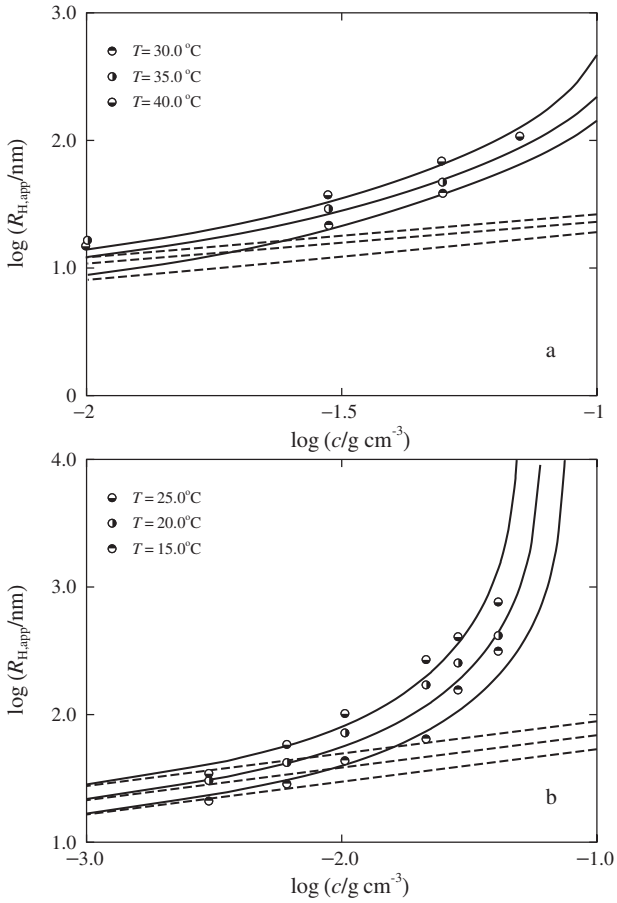

Figure 6. Bilogarithmic plots of $R_{H,app}$ against c for the $C_{10}E_6$ + n-dodecanol + water system of $w_d = 0.0704$ (a) and for the $C_{14}E_6$ + n-dodecanol + water system of $w_d = 0.0195$ (b) at various T indicated: the solid and dashed lines represent the theoretical values of $R_{H,app}$ and R_H for the isolated micelles, respectively.

25.0 °C, respectively. Figure 6 shows the results for the $C_{10}E_6$ micelles of $w_d = 0.0704$ at various T (a) and those for the $C_{14}E_6$ micelles of $w_d = 0.0195$ at various T (b), respectively. It is seen that at any given w_d and T, $R_{H,app}$ increases with increasing c. The increase of $R_{H,app}$ reflects both micellar growth in size and enhancement of the effects of the intermicellar hydrodynamic interactions with increasing c. $R_{H,app}$ as a function of c may be represented as

$$R_{H,app}(c) = R_H(c)H(c) \tag{13}$$

where $R_H(c)$ represents the hydrodynamic radius of a "isolated" micelle which may grow in size with c and $H(c)$ the hydrodynamic interactions which may be enhanced with c. In these two functions, $R_H(c)$ may be calculated by employing the equations formulated for the translational friction coefficient by Norisuye *et al.*[13] with wormlike spherocylinder model near the rod limit and by Yamakawa *et al.*[14,15] with the wormlike cylinder model, as a function of the micellar length L with including d and the stiffness parameter λ^{-1}. We are able to calculate $R_H(c)$ required in eq 13 as a function of c or M_w, by using eq 12. Here, L_w is used in place of L and the relation between M_w and c shown by the dashed lines in Figures 2 and 3 is utilized.

The function $H(c)$ in eq 13 may be calculated with the formulation given by Sato *et al.*[20–22] They have recently treated with the concentration dependence of the intermolecular hydrodynamic and direct collision interactions among wormlike polymer chains by using a fuzzy cylinder model. The fuzzy cylinder is defined as a cylinder which encapsulate a wormlike chain or a wormlike spherocylinder in the present case. Its effective length and diameter are evaluated from the wormlike chain parameters L, d, and λ^{-1}. Here, eq 12 and the experimental relationship between M_w and c are again utilized.

The solid curves in Figures 5 and 6 are the theoretical values of $R_{H,app}(c)$ thus calculated by eq 13 by

combining Sato *et al.*'s $H(c)$ with $R_H(c)$. Here, we have used the d values obtained from the analyses of the SLS data and determined the values of λ^{-1} so as to achieve the best fit to the observed results. As found in these Figures, the theoretical results are in good coincidence with the observed ones, although the data points are somewhat scattered. The increase of $R_{H,app}$ for the $C_{14}E_6$ micelles at large c seems to be too steep. It may come from the fact that the micelles grow in length with c to a extremely great extent as indicated below. The dashed lines represent relationships between R_H and c for the isolated micelles without any intermicellar hydrodynamic interaction, and thus the growth of the micelles with increasing c. We find that the solid and corresponding dashed lines, *i.e.*, $R_{H,app}(c)$ and $R_H(c)$, coincide with each other at small c and the difference between them becomes progressively large with c. The latter results imply that a great portion of $R_{H,app}$ results from the hydrodynamic interactions at large c and that the increase of the micellar size with c is rather moderate.

The λ^{-1} values obtained are 28, 38, and 50 nm for $w_d = 0.0306$, 0.0505, and 0.0704 at $T = 40.0\,^{\circ}C$, respectively, for the $C_{10}E_6$ micelles and 10, 11, 11, and 11 nm for $w_d = 0.0195$, 0.0368, 0.0406, and 0.0505 at $T = 25.0\,^{\circ}C$, respectively, for the $C_{14}E_6$ micelles. They were independent of temperature T except for the result for the $C_{10}E_6$ micelles with $w_d = 0.0704$ at $T = 30\,^{\circ}C$, which was $\lambda^{-1} = 140$ nm. The latter value is larger by a factor of 2.8 than the value at 40.0 °C. This may be due to the fact that the length of the $C_{10}E_6$ micelles is rather small at this low temperature. Another comment may be in order on the differences between the λ^{-1} values from $R_{H,app}$ and $\langle S^2 \rangle$ for the $C_{14}E_6$ micelles. The λ^{-1} values from $R_{H,app}$ are significantly smaller than those from $\langle S^2 \rangle$. These differences may be attributed to the fact that there is a distribution in micellar size and different averages are reflected in $R_{H,app}$ and $\langle S^2 \rangle$ as mentioned previously.[1,2,5] Recently, Sato has found that the distribution largely affects the evaluation of λ^{-1} from $\langle S^2 \rangle$ and that both of the λ^{-1} values from $\langle S^2 \rangle$ and R_H become comparable to each other when the effect of the micellar size distribution is taken into account.[31]

In Figures 7a, 7b, 8a, and 8b, the same observed and theoretical results for $R_{H,app}$ and R_H as those in Figures 5a, 5b, 6a, and 6b are shown as functions of M_w in the bilogarithmic plots, respectively. Here, the literature results for the $C_{10}E_6$[3] and $C_{14}E_6$[1] micelles with $w_d = 0$ are included in Figure 7a and b, respectively. The dashed lines represent the theoretical values of R_H and correspond to the relationship between R_H and M_w as usually shown for real polymer solutions. They asymptotically approach the data points and the solid curves as M_w is decreased, *i.e.*, as c is

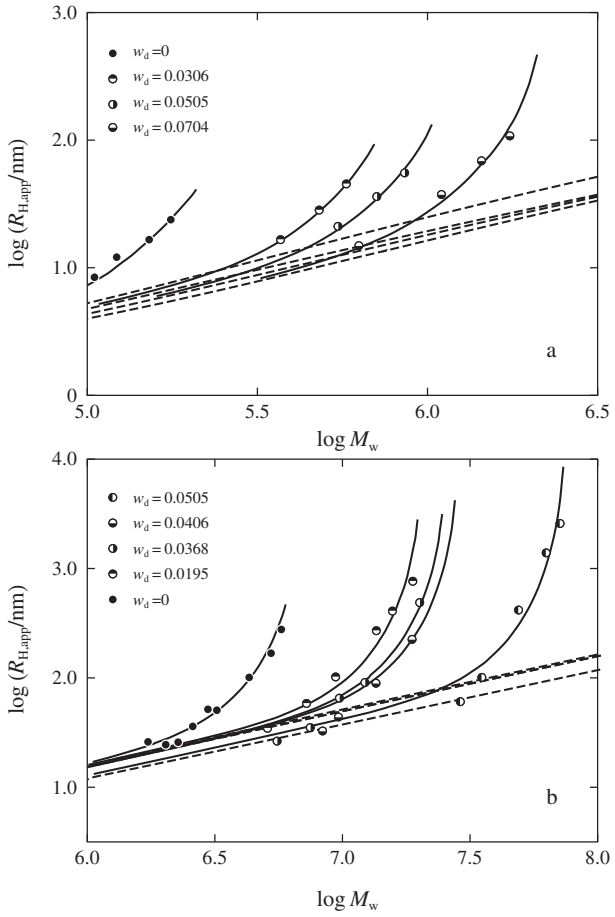

Figure 7. Bilogarithmic plots of $R_{H,app}$ against M_w for the $C_{10}E_6$ + *n*-dodecanol + water system ($T = 40.0\,^{\circ}C$) (a) and for the $C_{14}E_6$ + *n*-dodecanol + water system ($T = 25.0\,^{\circ}C$) (b) at various w_d indicated: the solid and dashed lines represent the theoretical values of $R_{H,app}$ and R_H for the isolated micelles, respectively.

lowered, indicating that the effects of the intermicellar hydrodynamic interactions on $R_{H,app}$ become negligible in the asymptotic region of low c. The results are in line with our previous findings for R_H of the single C_iE_j micelles.[1–3] At any given w_d at fixed T, the difference between the solid and dashed curves, which steeply increase with M_w, is due to the enhancement of the intermicellar hydrodynamic and dynamic interactions with increasing c, *i.e.*, the contribution of $H(c)$ to $R_{H,app}(c)$ in eq 13. In Figure 8a and b, the relations between R_H and M_w are represented by a respective single line (dashed line) except for the result for the $C_{10}E_6$ micelles at 30.0 °C (dotted line). The results comes from the fact that d and λ^{-1} for both micelles are independent of T and that for the $C_{10}E_6$ micelles at 30.0 °C, the λ^{-1} value is significantly larger than the one at higher T, as mentioned above.

The Micellar Length

Figure 9a and b depict the weight-average length

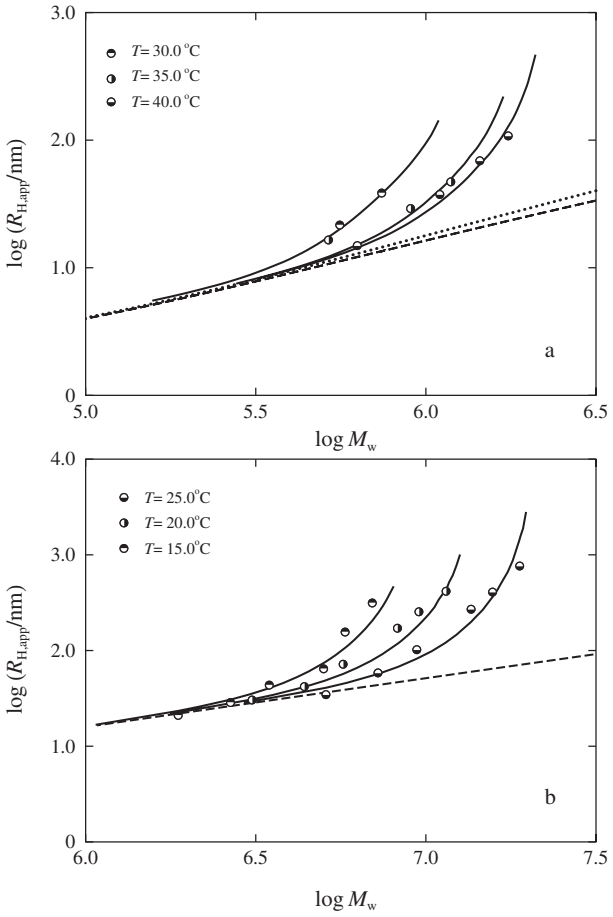

Figure 8. Bilogarithmic plots of $R_{H,app}$ against M_w for the $C_{10}E_6$ + *n*-dodecanol + water system of $w_d = 0.0704$ (a) and for the $C_{14}E_6$ + *n*-dodecanol + water system of $w_d = 0.0195$ (b) at various T indicated: the solid and dashed lines represent the theoretical values of $R_{H,app}$ and R_H for the isolated micelles, respectively.

L_w as a function of the surfactant weight fraction w_s and w_d for the $C_{10}E_6$ micelles at $T = 40.0\,^{\circ}C$ (a) and for the $C_{14}E_6$ micelles at 25.0 °C (b), respectively. Figure 10a and b show L_w as a function of w_s and T for the $C_{10}E_6$ micelles with $w_d = 0.0704$ (a) and for the $C_{14}E_6$ micelles with $w_d = 0.0195$ (b), respectively. Here, L_w has been calculated by eq 12 from the values of $M_w(c)$ and d obtained above from the analyses of the SLS data. It is found that the micelles at a given w_d (Figure 9) or T (Figure 10), L_w becomes larger as w_s is increased. As seen in these figures, L_w at fixed w_s steeply increases with increasing w_d, *i.e.*, with uptake of *n*-dodecanol into the micelles or with raising temperature.

We find that the $C_{14}E_6$ micelles grow in length to a greater extent than the $C_{10}E_6$ micelles. This finding is in line with our previous results[1–7] for the micelles of the single surfactant C_iE_j, in which the micelles formed with the surfactant molecules of the longer hydrophobic chain length have longer size.

Variation of Characteristics of the $C_{10}E_6$, $C_{12}E_6$, and $C_{14}E_6$ Micelles with uptake of n-Dodecanol

Figure 11 depicts w_d dependence of d for the $C_{10}E_6$ and $C_{14}E_6$ micelles containing *n*-dodecanol along with the previous results[17,18] for the $C_{12}E_6$ micelles containing *n*-dodecanol. The d values of these micelles increase with increasing *n*-dodecanol content in the micelles. It is found that for the $C_{14}E_6$ micelles, they increase with w_d gradually at small w_d and steeply at large w_d. The dependence of the d values on the hydrophobic chain length i of the surfactant molecules is not, however, systematic but roughly speaking, substantially independent of i.

Figure 12 illustrates w_d dependence of λ^{-1} evaluated from the analysis of the relationship between $R_{H,app}$ *vs* and c for the $C_{10}E_6$, $C_{12}E_6$, and $C_{14}E_6$ micelles containing *n*-dodecanol. The λ^{-1} values for any of the three micelles increase with increasing w_d. The increase is more significant for the micelles of the surfactant molecules with shorter hydrophobic chain length i. The value of λ^{-1} at fixed w_d is thus larger for the micelles of the surfactant molecules with smaller i. This result is in line with our previous results[5,7] for the micelles of the single surfactant C_iE_j, where the surfactant molecules of the shorter hydrophobic chain length form stiffer micelles.

CONCLUSIONS

In this work, we have examined variation of characteristics of the $C_{10}E_6$ and $C_{14}E_6$ micelles with uptake of *n*-dodecanol by static (SLS) and dynamic light scattering (DLS) measurements. As in the previous studies,[1–5,7–9,18,19] the SLS results $Kc/\Delta R_0$ have been successfully analyzed by the theory[10] for light scattering of micelle solutions formulated with wormlike spherocylinder model, to yield the molar mass $M_w(c)$ as a function of c along with the cross-sectional diameter d of the micelle. The mean-square radius of gyration $\langle S^2 \rangle$ as a function of M_w is well described by the Benoit-Doty equation[12] for the wormlike chain model. The apparent hydrodynamic radius $R_{H,app}(c)$ from DLS as a function of the micellar concentration has been also successfully analyzed by the fuzzy cylinder theory by Sato *et al.*[20–22] which takes into account the hydrodynamic and direct collision interactions among micelles and allowed us to evaluate the stiffness parameter λ^{-1}. The concentration c dependence of hydrodynamic radius $R_{H,app}$ was divided into two contributions: growth of the individual "isolated" micelles with c and enhancement of hydrodynamic and direct collision interactions among micelles with c.

The micellar length increases with increasing surfactant weight fraction w_s or with raising temperature T irrespective of the *n*-dodecanol content w_d. The

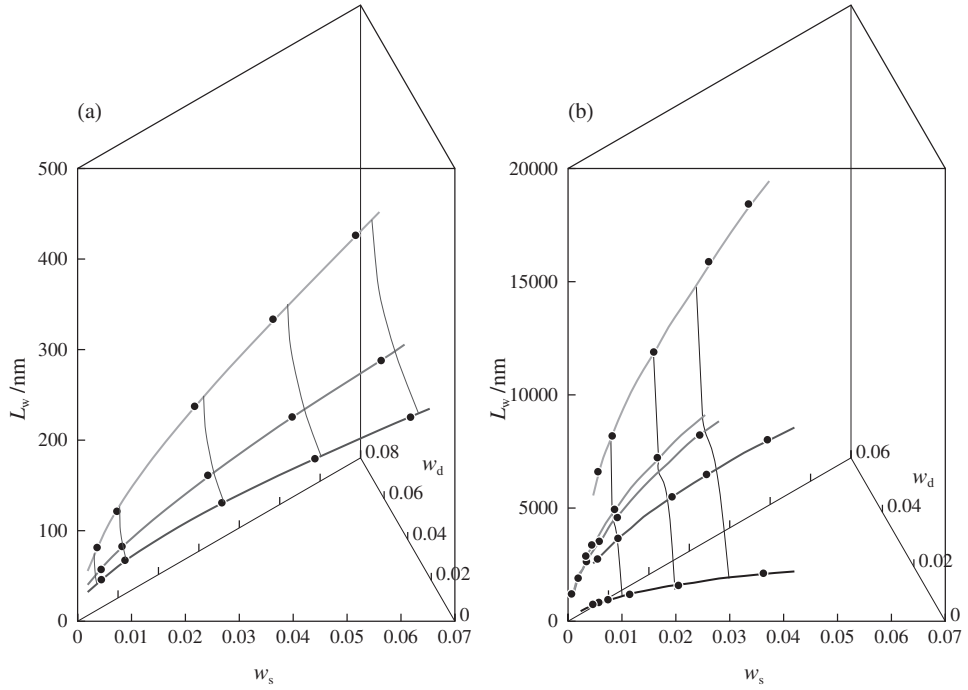

Figure 9. w_s and w_d dependence of the length L_w for the $C_{10}E_6$ + *n*-dodecanol micelles at 40.0 °C (a) and $C_{14}E_6$ + *n*-dodecanol micelles at 25.0 °C (b). Thick solid curves represent the results with decreasing order of w_d from top to bottom, respectively.

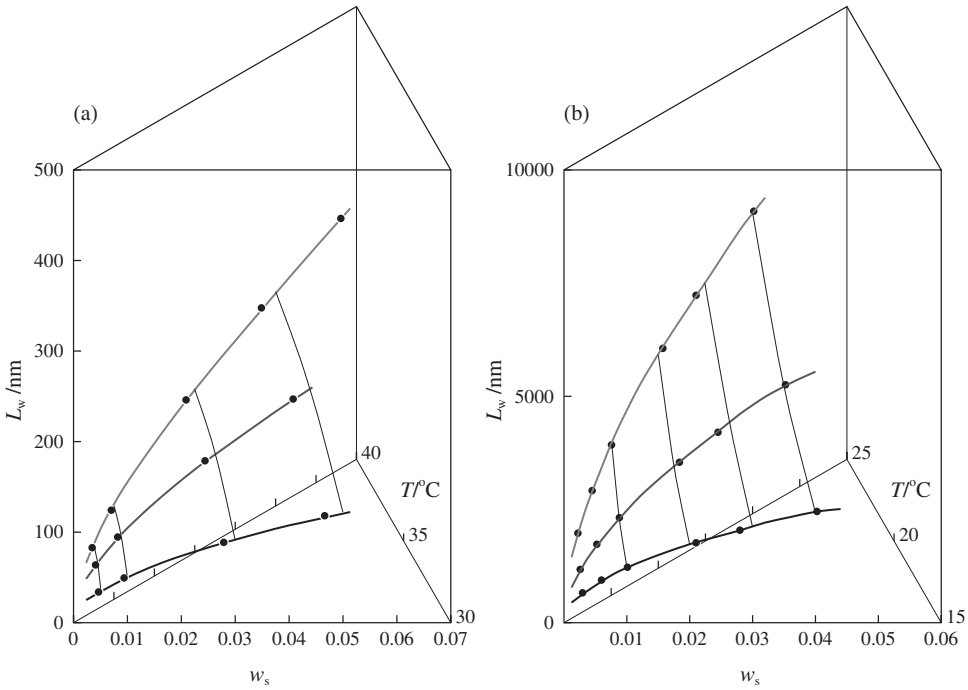

Figure 10. w_s and T dependence of the length L_w for the $C_{10}E_6$ + *n*-dodecanol micelles of $w_d = 0.0704$ (a) and $C_{14}E_6$ + *n*-dodecanol micelles of $w_d = 0.0195$ (b). Thick solid curves represent the results with decreasing order of T from top to bottom, respectively.

length of the micelles at fixed w_s and T steeply increases with increasing weight fraction w_d of *n*-dodecanol. The length of the $C_{14}E_6$ micelles is extremely larger than that of the $C_{10}E_6$ micelles. Both values of the cross-sectional diameter d and the stiffness parameter λ^{-1} increase with increasing w_d. It has been found that the increase in λ^{-1} is more significant for the micelles of the surfactant with shorter hydrophobic chain length.

Acknowledgment. The authors are grateful to Professor T. Sato of Osaka University for valuable discussions and providing us with the computer program to calculate the apparent hydrodynamic radius.

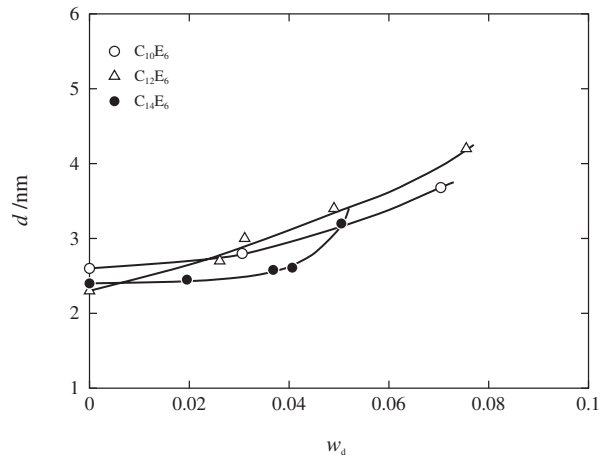

Figure 11. w_d dependence of the cross-sectional diameter d for the $C_{10}E_6$, $C_{12}E_6$, and $C_{14}E_6$ micelles containing *n*-dodecanol.

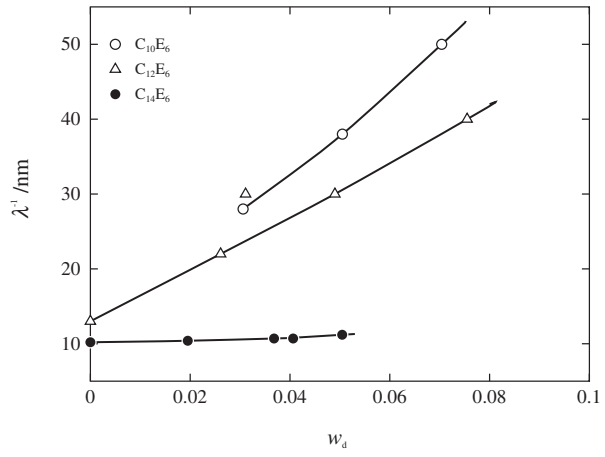

Figure 12. w_d dependence of the stiffness parameter λ^{-1} for the $C_{10}E_6$, $C_{12}E_6$, and $C_{14}E_6$ micelles containing *n*-dodecanol.

REFERENCES AND NOTES

1. S. Yoshimura, S. Shirai, and Y. Einaga, *J. Phys. Chem. B*, **108**, 15477 (2004).
2. N. Hamada and Y. Einaga, *J. Phys. Chem. B*, **109**, 6990 (2005).
3. K. Imanishi and Y. Einaga, *J. Phys. Chem. B*, **109**, 7574 (2005).
4. Y. Einaga, A. Kusumoto, and A. Noda, *Polym. J.*, **37**, 368 (2005).
5. S. Shirai and Y. Einaga, *Polym. J.*, **37**, 913 (2005).
6. S. Shirai, S. Yoshimura, and Y. Einaga, *Polym. J.*, **38**, 37 (2006).
7. Y. Einaga, Y. Inaba, and M. Syakado, *Polym. J.*, **38**, 64 (2006).
8. Y. Einaga, Y. Kito, and M. Watanabe, *Polym. J.*, **38**, 1267 (2006).
9. K. Imanishi and Y. Einaga, *J. Phys. Chem. B*, **111**, 62 (2007).
10. T. Sato, *Langmuir*, **20**, 1095 (2004).
11. R. Koyama and T. Sato, *Macromolecules*, **35**, 2235 (2002).
12. H. Benoit and P. Doty, *J. Phys. Chem.*, **57**, 958 (1953).
13. T. Norisuye, M. Motowoka, and H. Fujita, *Macromolecules*, **12**, 320 (1979).
14. H. Yamakawa and M. Fujii, *Macromolecules*, **6**, 407 (1973).
15. H. Yamakawa and T. Yoshizaki, *Macromolecules*, **12**, 32 (1979).
16. T. Yoshizaki, I. Nitta, and H. Yamakawa, *Macromolecules*, **21**, 165 (1988).
17. Y. Einaga, Y. Totake, and H. Matsuyama, *Polym. J.*, **36**, 971 (2004).
18. M. Miyake and Y. Einaga, *J. Phys. Chem. B*, **111**, 535 (2007).
19. M. Miyake and Y. Einaga, *Polym. J.*, submitted.
20. T. Kanematsu, T. Sato, Y. Imai, K. Ute, and T. Kitayama, *Polym. J.*, **37**, 65 (2005).
21. A. Ohshima, A. Yamagata, T. Sato, and A. Teramoto, *Macromolecules*, **32**, 8645 (1999).
22. T. Sato, A. Ohshima, and A. Teramoto, *Macromolecules*, **31**, 3094 (1998).
23. B. Berne and R. Pecora, "Dynamic Light Scattering," J. Wiley, New York, 1976.
24. H. Vink, *J. Chem. Soc., Faraday Trans. I*, **81**, 1725 (1985).
25. P. Štěpánek, W. Brown, and S. Hvidt, *Macromolecules*, **29**, 8888 (1996).
26. D. Blankschtein, G. M. Thurston, and G. B. Benedek, *J. Chem. Phys.*, **85**, 7268 (1986).
27. M. E. Cates and S. J. Candau, *J. Phys.: Condens. Matter*, **2**, 6869 (1990).
28. N. Zoeller, L. Lue, and D. Blankschtein, *Langmuir*, **13**, 5258 (1997).
29. E. F. Casassa and G. C. Berry, "Polymer Solutions. In Comprehensive Polymer Science," G. Allen, Ed., Pergamon Press, New York, 1988.
30. G. C. Berry, *Adv. Polym. Sci.*, **1994**, *114*, 233.
31. T. Sato, *Private Communication*.